Optimising NMR Spectroscopy through Method and Software Development (?)

Jonathan Yong

University of Oxford

Contents

Abstract

I did stuff

Preface

Pulse sequence notation

Filled black rectangular bars indicate 90° pulses; empty bars indicate 180° pulses. Pulses with other flip angles are depicted using filled grey bars, typically with the Greek letter β above it representing the flip angle. Delays are variously represented by the letters Δ and τ, and phases by ϕ; exact values of these are given in the respective captions. Decaying sinusoids mark detection periods, sometimes with simultaneous heteronuclear decoupling on other channels (grey boxes labelled 'dec.'). z-Gradient amplitudes are given as percentages of the maximum gradient amplitude, which is probehead-dependent (see table 0.1). This maximum amplitude is unlikely to substantially affect the performance of any of the pulse sequences; consequently, I quote gradient amplitudes only as percentages. In practice, pulse programmes may be implemented with tiny differences in delays to accommodate finite pulse widths and other technicalities.

Samples used

The caption of every figure showing experimental data includes a 'code' at the end, which indicates the spectrometer and sample used for the data. These possibilities are enumerated in tables 0.1 and 0.2 and fig. 0.1. Therefore, for example, the code `7Z` would represent data acquired on the 700 MHz spectrometer on the zolmitriptan sample.

Software

All NMR data was processed using TopSpin 3 or 4. Quantum mechanical NMR simulations were done in Matlab R2021a or R2021b. This thesis is written using the LaTeX typesetting system: specifically, I used the LuaLaTeX engine.

Pulse sequences are drawn using the vector graphics programme Inkscape. Plots are generated using Python 3, using a number of packages (namely: `numpy`, `scipy`, `matplotlib`, `seaborn`, and

Code	Internal name	Details
7	AV700	700 MHz ^{1}H resonance frequency 5 mm TCI ^{1}H/^{13}C/^{15}N inverse cryoprobe 53 G cm^{-1} maximum *z*-gradient amplitude AVANCE III console, TopSpin 3.6.2
6	AV600	600 MHz ^{1}H resonance frequency 5 mm Prodigy N_2 broadband cryoprobe (^{1}H/^{19}F outer coil) 66 G cm^{-1} maximum *z*-gradient amplitude AVANCE III console, TopSpin 3.6.2
4	AVB400	400 MHz ^{1}H resonance frequency 5 mm broadband (room-temperature) SmartProbe 50 G cm^{-1} maximum *z*-gradient amplitude AVANCE NEO console, TopSpin 4.0.8

Table 0.1: Spectrometers used in this thesis. A more complete description may be accessed via the links in the 'internal name' column.

Code	Compound	Solvent	Concentration
A	Andrographolide	DMSO-d_6	40 mM
B	(3-Fluorophenyl)boronic acid	DMSO-d_6	120 mM
C	Cyclosporin A	C_6D_6	50 mM
E	Ethanol	D_2O	1 M
F	Ferulic acid	DMSO-d_6	50 mM
G	Gramicidin S	DMSO-d_6	40 mM
H	Cholesterol	$CDCl_3$	50 mM
S	Sucrose	90% H_2O / 10% D_2O	22 mM
T	Ethyl ferulate	DMSO-d_6	200 mM
X	Brucine	$CDCl_3$	50 mM
Z	Zolmitriptan	DMSO-d_6	50 mM

Table 0.2: Samples used in this thesis. Note that concentrations are approximate and not necessarily constant, as samples were remade over time due to e.g. decomposition. However, it is reasonable to assume that the variation in concentration is below 10%. See fig. 0.1 for chemical structures.

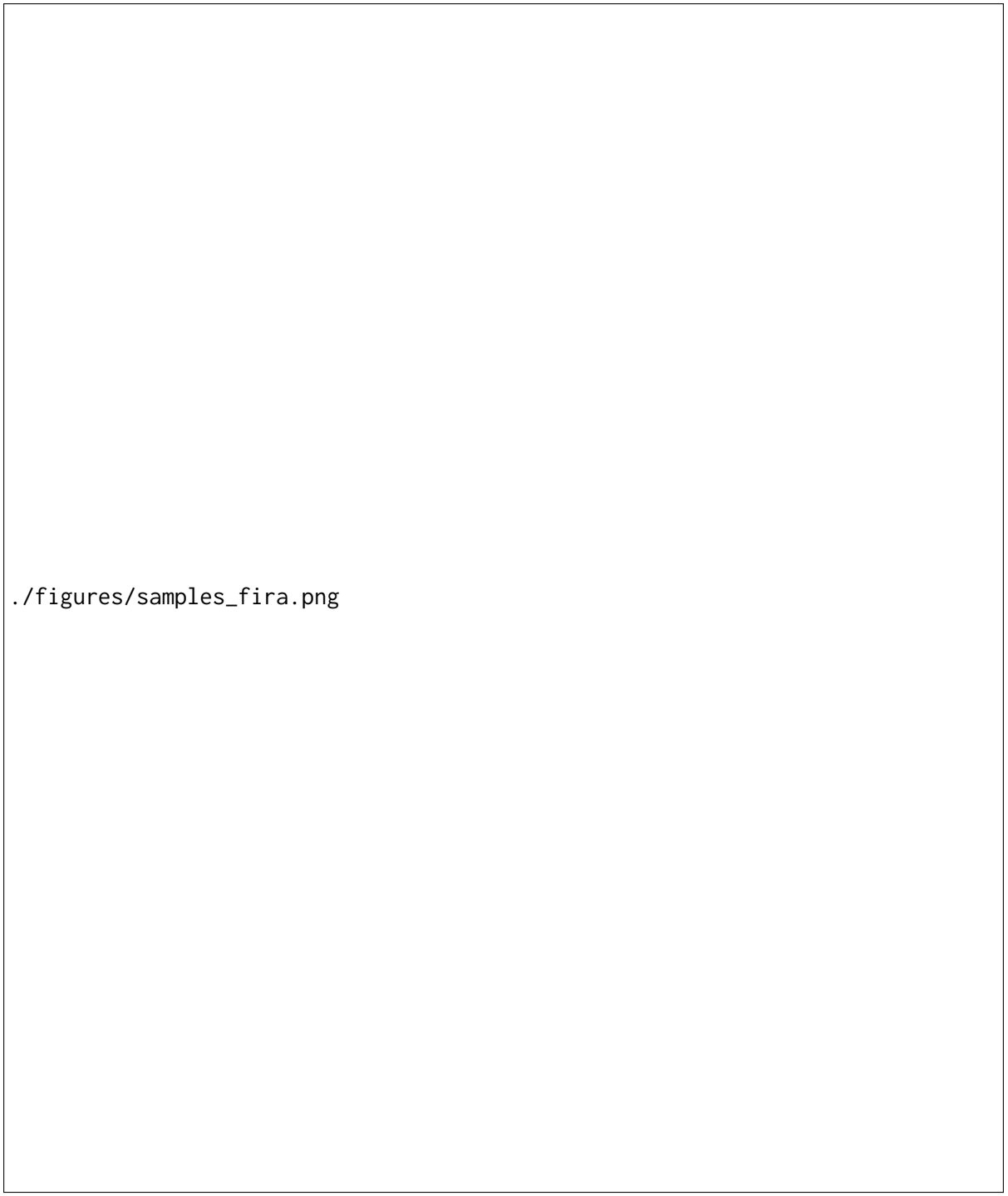

Figure 0.1: Chemical structures of samples used in this thesis. See table 0.2 for more information.

`penguins`, the last of which was written by me, and described further in appendix A.1). Even if the underlying data was generated in Matlab, I have invariably opted to export it (e.g., to a CSV file) and plot it using Python.

The underlying LaTeX code for this thesis, as well as all figures, can be accessed at TODO (likely GitHub).

Acknowledgements

A quote goes here

By somebody

Thanks

Chapter 1

NMR theory

I begin with an overview of basic NMR theory, specifically, the dynamics of quantum systems containing one or more spin-½ particles. Note that this is not designed to be an exhaustive account (many textbooks are available for this purpose[1–5]).

1.1 Quantum mechanics

The most fundamental equation in (non-relativistic) quantum mechanics, which governs the time evolution of a state $|\Psi(t)\rangle$, is the time-dependent Schrödinger equation:

$$\frac{\partial|\Psi(t)\rangle}{\partial t} = -\frac{\mathrm{i}}{\hbar}H|\Psi(t)\rangle \tag{1.1}$$

For a Hamiltonian H which does not change during a period of time $t_1 \leq t \leq t_2$ (i.e. is *time-independent*), this can be integrated to yield an explicit solution:

$$|\Psi(t_2)\rangle = \exp\left[-\frac{\mathrm{i}H(t_2 - t_1)}{\hbar}\right]|\Psi(t_1)\rangle \tag{1.2}$$

The term $\exp[-\mathrm{i}H(t_2 - t_1)/\hbar]$ is called the *propagator* of the system and denoted $U(t_2, t_1)$; this is often further simplified to $U(\tau)$ where $\tau = t_2 - t_1$ is the duration of the evolution. For a Hamiltonian which varies with time but is piecewise constant, in that it can be broken up into several finite periods within which H is time-independent, the time evolution of the state is simply given by successive application of propagators:

$$|\Psi(t_n)\rangle = U(t_n, t_{n-1}) \cdots U(t_2, t_1)U(t_1, t_0)\,|\Psi(t_0)\rangle \tag{1.3}$$

assuming that $t_n > t_{n-1} > \cdots > t_0$. The case where H continuously varies with time is more complicated, but is not generally of interest in NMR and is thus not considered here.

In NMR, it is conventional to use units of angular frequencies instead of energies, for example by replacing $H/\hbar \to H$; this will henceforth be assumed. We now look at the specific forms of the Hamiltonians under consideration, i.e., the various nuclear spin interactions. The present work is restricted to systems with spin quantum number $I = 1/2$: these are two-level systems, where the eigenstates of I_z (denoted as $|\alpha\rangle$ and $|\beta\rangle$ for $m_I = +1/2$ and $-1/2$ respectively) are used as a standard basis. In this basis, the angular momentum operators take the following matrix representations:

$$I_x = \frac{1}{2}\begin{pmatrix} 0 & 1 \\ 1 & 0 \end{pmatrix}; \quad I_y = \frac{1}{2}\begin{pmatrix} 0 & -\mathrm{i} \\ \mathrm{i} & 0 \end{pmatrix}; \quad I_z = \frac{1}{2}\begin{pmatrix} 1 & 0 \\ 0 & -1 \end{pmatrix} \tag{1.4}$$

At this point, it is also useful to define the following linear combinations:

$$\begin{aligned} I_+ &= I_x + \mathrm{i}I_y = \begin{pmatrix} 0 & 1 \\ 0 & 0 \end{pmatrix}; \quad I_\alpha = \frac{1}{2}E + I_z = \begin{pmatrix} 1 & 0 \\ 0 & 0 \end{pmatrix} \\ I_- &= I_x - \mathrm{i}I_y = \begin{pmatrix} 0 & 0 \\ 1 & 0 \end{pmatrix}; \quad I_\beta = \frac{1}{2}E - I_z = \begin{pmatrix} 0 & 0 \\ 0 & 1 \end{pmatrix} \end{aligned} \tag{1.5}$$

where E is the 2×2 identity matrix. The *coherence order* of an operator, denoted p, is defined by the states it connects, i.e. the nonzero elements in its matrix form: an operator $O = |m_2\rangle\langle m_1|$ would represent $(m_2 - m_1)$-order coherence, since $\langle m_2|O|m_1\rangle \neq 0$. Thus, in the above equations, I_+ represents a coherence order of $+1$; I_- a coherence order of -1; I_x and I_y are both a mixture of ± 1-coherence; and the remainder have coherence order 0.

States (and operators) for composite systems are defined as tensor products of single-spin states (and operators);[6] in matrix form, these can be expressed using the Kronecker product.[5] Thus, for example, the operator $2I_xS_z$ could be represented as follows:*

$$2I_xS_z = 2 \cdot \frac{1}{2} \cdot \frac{1}{2}\left[\begin{pmatrix} 0 & 1 \\ 1 & 0 \end{pmatrix} \otimes \begin{pmatrix} 1 & 0 \\ 0 & -1 \end{pmatrix}\right] = \frac{1}{2}\begin{pmatrix} 0 & 0 & 1 & 0 \\ 0 & 0 & 0 & -1 \\ 1 & 0 & 0 & 0 \\ 0 & -1 & 0 & 0 \end{pmatrix} \tag{1.6}$$

The Hamiltonians H for multiple-spin systems are formed from such operators. It is useful to

*This representation is not unique; it is perfectly possible to reverse the order of the Kronecker product, and as long as this is consistently done, any physically measurable quantities calculated using this alternative will be the same.

'decompose' H into different interactions.[3] In solution-state NMR, these interactions include:

$$H_{\text{cs}} = \sum_i \omega_{0,i} I_{iz} \qquad \text{(chemical shift)} \tag{1.7}$$

$$H_{\text{J}} = \sum_{i>j} 2\pi J_{ij} (\mathbf{I}_i \cdot \mathbf{I}_j) \qquad \text{(scalar coupling)} \tag{1.8}$$

$$H_{\text{pulse}} = \sum_i \omega_{i,x} I_{ix} + \sum_i \omega_{i,y} I_{iy} \qquad \text{(radiofrequency pulses)} \tag{1.9}$$

$$H_{\text{grad}} = \sum_i \gamma_i G z I_{iz} \qquad \text{(pulsed field gradients on } z\text{)} \tag{1.10}$$

Pulsed field gradients (henceforth shortened to *gradients*) can in principle be applied along any axis, not just z, but this is dependent on hardware: all the work in this thesis was done on z-gradient probes. In the above expressions:

- γ_i is the magnetogyric ratio of spin i;
- $\omega_{0,i}$ refers to the Larmor, or precession, frequency of spin i (usually on the order of MHz). The Larmor frequency is defined as

$$\omega_{0,i} = -\gamma_i B_0, \tag{1.11}$$

  where B_0 is the strength of the external (static) magnetic field;
- J_{ij} is the scalar coupling constant between spins i and j (expressed in units of Hz);
- ω_x and ω_y are amplitudes of radiofrequency (RF) pulses along the x- and y-axes, which are in general time-dependent, and are related to the so-called B_1 by a factor of γ_i.
- G is the amplitude of the gradient, typically in units of G/cm; and
- z is the position of the spin along the z-axis, typically in units of cm.

Finally, note that in the *weak coupling* regime where

$$\omega_{0,i} - \omega_{0,j} \gg J_{ij}, \tag{1.12}$$

the scalar coupling Hamiltonian may be simplified (the *secular approximation**) to

$$H_{\text{J,secular}} = \sum_{i>j} 2\pi J_{ij} I_{iz} I_{jz}. \tag{1.13}$$

*This result comes from the use of time-independent nondegenerate perturbation theory: it is based on the assumption that the eigenstates $\{|n\rangle\}$ of the main Hamiltonian H_0 are unchanged by the perturbation V (since the first-order correction varies as $\sum_m V_{mn}/(\omega_m - \omega_n) \ll 1$), and only the first-order correction to the energies $E_n^{(1)} = \langle n|V|n\rangle$ is retained. In this context, H_0 and V are respectively H_{cs} and H_{J}. When the condition eq. (1.12) does not hold, the nondegenerate treatment fails; see e.g. Sakurai.[6]

This condition is always satisfied whenever spins i and j are different nuclides.

Throughout the course of an NMR experiment, RF pulses and gradients are turned on and off, and thus H_{pulse} and H_{grad} are time-dependent—although they will always satisfy the 'piecewise constant' criterion which allows us to use eq. (1.3). The 'free precession' (or simply 'free') Hamiltonian, H_{free}, refers to the active Hamiltonian whenever no pulses or gradients are being applied:

$$H_{\text{free}} = H_{\text{cs}} + H_{\text{J}}. \tag{1.14}$$

This is always time-independent as these correspond to physical parameters which cannot be changed.

1.2 The rotating frame

The Hamiltonians described above refer to the 'laboratory frame' or the *Schrödinger picture*, where spins precess about the z-axis at their intrinsic frequencies and obey the equation of motion (1.1). However, this proves to often be unwieldy, in particular when analysing the effects of radiofrequency pulses. It is standard procedure to transform the frame of reference to a 'rotating frame', specifically, one which rotates about the z-axis at a defined rotation frequency ω_{rot} which is close to the Larmor frequencies ω_0.

The rotating frame can be formalised using the *interaction picture* of quantum mechanics,[6] which involves the separation of the Hamiltonian into two parts, with the first typically being completely time-independent:

$$H(t) = H_0 + H_1(t). \tag{1.15}$$

In this case, the static part H_0 simply corresponds to precession of the spins at a particular frequency:

$$H_0 = \sum_i \omega_{\text{rot},i} I_{iz}. \tag{1.16}$$

(Generally, each instance of the same nuclide (e.g. ^{1}H or ^{13}C) will share the same ω_{rot}, so the subscript $\omega_{\text{rot},i}$ is useful only to distinguish different nuclear species.) This allows us to define H_1 as

$$\begin{aligned} H_1 &= H_{\text{J}} + H_{\text{pulse}} + H_{\text{grad}} + (H_{\text{cs}} - H_0) \\ &= H_{\text{J}} + H_{\text{pulse}} + H_{\text{grad}} + \sum_i \Omega_i I_{iz} \\ &= H_{\text{J}} + H_{\text{pulse}} + H_{\text{grad}} + H_{\text{offset}} \end{aligned} \tag{1.17}$$

where $\Omega_i = \omega_{0,i} - \omega_{\text{rot},i}$ is the *offset* of spin i. For reasons which will become clear later, the

frequency ω_{rot} is chosen to be the centre of the spectral window for the given nuclide.

Having split up our Hamiltonian, we then define an *interaction-picture ket*:

$$|\Psi\rangle_I = \exp(\mathrm{i}H_0 t)\,|\Psi\rangle\,. \tag{1.18}$$

The time evolution of this ket is given by a transformation of the Schrödinger equation:

$$\begin{aligned}
\frac{\partial|\Psi\rangle_I}{\partial t} &= \mathrm{i}H_0\exp(\mathrm{i}H_0 t)\,|\Psi\rangle + \exp(\mathrm{i}H_0 t)\frac{\partial|\Psi\rangle}{\partial t} \\
&= \mathrm{i}H_0\,|\Psi\rangle_I + \exp(\mathrm{i}H_0 t)(-\mathrm{i}H|\Psi\rangle) \\
&= \mathrm{i}H_0\,|\Psi\rangle_I - \mathrm{i}\exp(\mathrm{i}H_0 t)(H_0+H_1)\exp(-\mathrm{i}H_0 t)\,|\Psi\rangle_I \\
&= \mathrm{i}H_0\,|\Psi\rangle_I - \mathrm{i}H_0\,|\Psi\rangle_I - \mathrm{i}\exp(\mathrm{i}H_0 t)H_1\exp(-\mathrm{i}H_0 t)\,|\Psi\rangle_I \\
&= -\mathrm{i}\exp(\mathrm{i}H_0 t)H_1\exp(-\mathrm{i}H_0 t)\,|\Psi\rangle_I \\
&= -\mathrm{i}H_{1,I}|\Psi\rangle_I\,,
\end{aligned} \tag{1.19}$$

where

$$H_{1,I} = \exp(\mathrm{i}H_0 t)H_1\exp(-\mathrm{i}H_0 t). \tag{1.20}$$

The underlying principle here is that the 'interesting' behaviour should be contained in H_1 (or rather $H_{1,I}$), and the interaction-picture states $|\Psi\rangle_I$ only evolve under this term. The effect of H_0 is not neglected, but rather it is 'absorbed' into the operators instead of the ket (eq. (1.20)).

We now turn our attention to how the various NMR Hamiltonians (eqs. (1.7) to (1.10)) are transformed in the interaction picture; that is to say, what the individual terms in the rhs of

$$\begin{aligned}
H_{1,I} = {}& \exp(\mathrm{i}H_0 t)H_{\text{J}}\exp(-\mathrm{i}H_0 t) + \exp(\mathrm{i}H_0 t)H_{\text{pulse}}\exp(-\mathrm{i}H_0 t) \\
&+ \exp(\mathrm{i}H_0 t)H_{\text{grad}}\exp(-\mathrm{i}H_0 t) + \exp(\mathrm{i}H_0 t)H_{\text{offset}}\exp(-\mathrm{i}H_0 t)
\end{aligned} \tag{1.21}$$

are. We first note that H_0 (and hence $\exp(\pm\mathrm{i}H_0 t)$) is a function only of the I_{iz} operators; thus, any Hamiltonian which commutes with all I_{iz}'s will be untouched by this transformation. This is trivially true of H_{offset} and H_{grad}, which are themselves both functions of the I_{iz}'s. It can also be shown that H_{J} (in the homonuclear case) and $H_{\text{J,secular}}$ (heteronuclear case) fully commute with H_0. So, for three out of the four terms in eq. (1.21) we simply have the result that $\exp(\mathrm{i}H_0 t)H\exp(-\mathrm{i}H_0 t) = H$. This allows us to immediately write down the free precession Hamiltonian in the interaction picture:

$$H_{\text{free},I} = H_{\text{offset}} + H_{\text{J}}. \tag{1.22}$$

The fourth term, which does not commute with H_0, is H_{pulse}. In the laboratory frame, *hard pulses*

are applied as oscillating RF fields. Consider the case of a pulse acting on a single spin:

$$H_{\text{pulse,hard}} = \omega_1[\cos(\omega_{\text{rf}}t + \phi)I_x + \sin(\omega_{\text{rf}}t + \phi)I_y]. \tag{1.23}$$

Here, ω_1 represents the *amplitude* of the pulse, and ϕ the *phase*. This expression is similar to the expression in eq. (1.9), but here ω_1 and ϕ are both constants, with the time dependence explicitly specified using the *frequency* of the pulse, ω_{rf}. In the rotating frame, using that $H_0 = \omega_{\text{rot}}I_z$, we then have the following interaction Hamiltonian:

$$\begin{aligned} H_{\text{pulse,hard},I} = \omega_1 \big[&\exp(\mathrm{i}\omega_{\text{rot}}tI_z)I_x \cos(\omega_{\text{rf}}t + \phi) \exp(-\mathrm{i}\omega_{\text{rot}}tI_z) \\ &+ \exp(\mathrm{i}\omega_{\text{rot}}tI_z)I_y \sin(\omega_{\text{rf}}t + \phi) \exp(-\mathrm{i}\omega_{\text{rot}}tI_z)\big], \end{aligned} \tag{1.24}$$

and using the formulae

$$\exp(\mathrm{i}\theta I_z)I_x \exp(-\mathrm{i}\theta I_z) = I_x \cos\theta - I_y \sin\theta \tag{1.25}$$

$$\exp(\mathrm{i}\theta I_z)I_y \exp(-\mathrm{i}\theta I_z) = I_y \cos\theta + I_x \sin\theta \tag{1.26}$$

(see Appendix A.2 of Levitt[3] for a derivation), eq. (1.24) simplifies to

$$H_{\text{pulse,hard},I} = \omega_1 \left[I_x \cos(\omega_{\text{rf}} - \omega_{\text{rot}} + \phi) + I_y \sin(\omega_{\text{rf}} - \omega_{\text{rot}} + \phi)\right]. \tag{1.27}$$

The frequency at which hard pulses are applied is termed the *transmitter frequency*, ω_{tx}. This is a parameter which can be controlled by the user, and is typically placed in the centre of the spectrum of the sample under study, in order to make the most use of its *bandwidth* (the region of frequencies over which the pulse is effective). For convenience, it is then typical to then choose the rotating-frame frequency to be exactly the same frequency: $\omega_{\text{rot}} = \omega_{\text{tx}}$ This allows us to simplify the rotating-frame Hamiltonian to

$$H_{\text{pulse,hard},I} = \omega_1(I_x \cos\phi + I_y \sin\phi), \tag{1.28}$$

which is time-*independent*. Occasionally, I will also use the Cartesian components:

$$(c_x, c_y) = (\omega_1 \cos\phi, \omega_1 \sin\phi), \tag{1.29}$$

instead of the amplitude and phase, to describe the pulse.

Consider now the application of this pulse to an isolated spin for which $\omega_0 = \omega_{\text{rot}}$ and thus has an offset $\Omega = 0$. We have that $H_{\text{offset}} = H_{\text{J}} = H_{\text{grad}} = 0$, and the only active Hamiltonian is that of the pulse, which causes *nutation* of the spin magnetisation vector around the axis of the pulse;

in this case, the pulse (or the spin) is said to be *on-resonance*.* If a duration for the pulse τ_p is further specified, this also allows us to define a *flip angle* $\beta = \omega_1 \tau_p$. On the other hand, spins which are *off-resonance* ($\omega_0 - \omega_{tx} \neq 0$) evolve not only under the pulse Hamiltonian but also the offset; this leads to a different effective flip angle and axis of rotation. Off-resonance effects may be neglected when considering an idealised, infinitely hard pulse. However, this is of course not possible on a spectrometer, and in practice off-resonance effects are noticeable even for hard pulses as short as several microseconds.

In general, RF pulses are more complicated than the simple case of the hard pulse shown here. For example, they may be constructed such that even in the rotating frame there is still a time dependence in the amplitudes and/or the phases; these are often referred to as *shaped*, *amplitude-modulated*, or *frequency-modulated* pulses depending on the context. In principle, ω_1 and ϕ may both be continuous functions of time; however, for ease of construction and implementation, pulses are typically generated in a *piecewise* or discrete method using n points each of time δt, within which ω_1 and ϕ (or equivalently, c_x and c_y) are constant. The total length of the pulse is then simply $n(\delta t)$; δt is sometimes called the *timestep* of the pulse.

1.3 Density operators

NMR experiments are not executed on one single spin at a time: instead, the samples used typically contain $\sim 10^{20}$ spins. Furthermore, each of these spins may have its own wavefunction: it is generally impossible to force every spin to possess the same state. Since we are only interested in the *ensemble* behaviour such as expectation values, rather than the dynamics of each individual spin, we can use the *density operator* formalism instead of dealing with a composite wavefunction of many spins. The density operator, ρ, is defined (in the Schrödinger picture) as

$$\rho = \sum_j p_j |\psi_j\rangle \langle\psi_j| \tag{1.30}$$

where p_j is the probability that a spin is in the state $|\psi_j\rangle$ (and the $|\psi_j\rangle$'s are assumed to form a complete set of states).† The use of ρ actually represents a loss of information, in that while eq. (1.30) gives us a straightforward recipe for constructing ρ from a given distribution of states $\{p_j, |\psi_j\rangle\}$, the reverse is not possible: given a known ρ, it is generally not possible to determine a

*Strictly speaking, the rotating frame is just a mathematical formalism, so the resonance condition does not necessitate $\Omega = 0$ or $\omega_{rf} = \omega_{rot} = \omega_0$. We only need that $\omega_{rf} = \omega_0$, or in other words, that the pulse is applied at the frequency of the spin—which may or may not be the same as the rotating-frame frequency. Practically, such a situation may arise in (for example) the application of selective pulses to a specific spin which is not at the centre of the spectrum.

†This probability is a *classical* probability: that is, it is purely statistical in nature and should not be confused with the probability amplitudes associated with quantum superposition (i.e. $|c_j|^2$ in a single-spin wavefunction $\sum_j c_j |j\rangle$).

unique distribution of states. This is not a problem, however, because ρ contains all the necessary information for calculation of expectation values, in that for any operator A,

$$\langle A \rangle = \sum_j \langle \psi_j | A \rho | \psi_j \rangle \,. \tag{1.31}$$

If A and ρ are expressed as matrices (through any choice of basis), then this is more easily expressed as the trace of the matrix product:

$$\langle A \rangle = \mathrm{Tr}(A\rho). \tag{1.32}$$

Other properties of the density operator are not discussed here, but can be found in virtually any textbook covering their use.[6–8]

The time evolution of a Schrödinger-picture density operator is governed by the Liouville–von Neumann equation, which can be derived from eq. (1.1):

$$\begin{aligned}
\frac{\mathrm{d}\rho}{\mathrm{d}t} &= \sum_j p_j \left(\frac{\mathrm{d}\,|\psi_j\rangle}{\mathrm{d}t} \langle \psi_j| + |\psi_j\rangle \frac{\mathrm{d}\,\langle \psi_j|}{\mathrm{d}t} \right) \\
&= \sum_j p_j \left(-\mathrm{i}H |\psi_j\rangle \langle \psi_j| + |\psi_j\rangle \,\mathrm{i} \langle \psi_j| H \right) \\
&= -\mathrm{i}H \left(\sum_j p_j \,|\psi_j\rangle \langle \psi_j| \right) + \mathrm{i} \left(\sum_j p_j \,|\psi_j\rangle \langle \psi_j| \right) H \\
&= -\mathrm{i}[H, \rho].
\end{aligned} \tag{1.33}$$

Note here that the weights p_j are time-independent, as the time evolution is contained entirely in the kets and bras.* For a time-independent H, this can be integrated to yield the solution:

$$\rho(t_2) = \exp(-\mathrm{i}H\tau)\rho(t_1)\exp(\mathrm{i}H\tau), \tag{1.34}$$

where $\tau = t_2 - t_1$.

In the interaction picture, the density operator is instead defined using interaction-picture states

*Strictly speaking, this only applies to a *closed* quantum system, which implies that effects such as relaxation are ignored (or at least, treated in only an empirical manner). The discussion of open quantum systems is beyond the scope of this work, but can be found elsewhere.[9,10]

$\{|\psi_i\rangle_I\}$:

$$\begin{aligned}\rho_I = \sum_j p_j |\psi_j\rangle_I \langle\psi_j|_I &= \sum_j p_j \exp(\mathrm{i}H_0 t)\,|\psi_j\rangle\,\langle\psi_j|\exp(-\mathrm{i}H_0 t) \\ &= \exp(\mathrm{i}H_0 t)\left(\sum_j p_j |\psi_j\rangle\langle\psi_j|\right)\exp(-\mathrm{i}H_0 t) \\ &= \exp(\mathrm{i}H_0 t)\rho\exp(-\mathrm{i}H_0 t) \end{aligned} \tag{1.35}$$

(note the similarity to eq. (1.20)). Using a very similar proof as in eq. (1.33), it can be shown that ρ_I obeys a modified Liouville–von Neumann equation:

$$\frac{\mathrm{d}\rho_I}{\mathrm{d}t} = -\mathrm{i}[H_{1,I}, \rho_I] \tag{1.36}$$

and analogously, for a time-independent $H_{1,I}$ we have that

$$\rho_I(t_2) = \exp(-\mathrm{i}H_{1,I}\tau)\rho_I(t_1)\exp(\mathrm{i}H_{1,I}\tau) = U\rho_I(t_1)U^\dagger, \tag{1.37}$$

where $U = \exp(-\mathrm{i}H_{1,I}\tau)$. Multiple propagators may be chained in a similar fashion to eq. (1.3). This result means that from a practical point of view, the effects of H_0 can be completely ignored when analysing or simulating NMR experiments using density operators.

Finally, a mention of the *equilibrium* or *thermal* density operator is in order. For a canonical ensemble, this is given by:

$$\rho_0 = \frac{\exp(-\beta\hbar H)}{\mathrm{Tr}[\exp(-\beta\hbar H)]} \tag{1.38}$$

where $\beta = 1/(k_\mathrm{B}T)$ and the Hamiltonian H is in units of angular momentum, as has been consistently used here. At equilibrium, no pulses or gradients are being applied, so the appropriate Hamiltonian is the free (Schrödinger-picture) Hamiltonian H_free (eq. (1.14)).* Consider the case of a single spin: we have that $H_\mathrm{J} = 0$, and hence $H_\mathrm{free} = H_\mathrm{cs} = \omega_0 I_z$. Thus,

$$\rho_0 = \frac{\exp(cI_z)}{\mathrm{Tr}[\exp(cI_z)]} \approx \frac{E + cI_z}{\mathrm{Tr}(E + cI_z)} = E + cI_z, \tag{1.39}$$

where $c = -\beta\hbar\omega_0 = -\hbar\omega_0/k_\mathrm{B}T$ and E is the identity matrix; the approximation $\exp(cI_z) \approx E + cI_z$ is justified here as c is typically very small ($\sim 10^{-5}$).

Throughout this thesis I consider only linear transformations of the form in eq. (1.37), which use

*It would be completely insensible to use the interaction-picture $H_{\mathrm{free},I}$, as its entire existence is merely a mathematical formalism. If that were not the case, it would imply that we can change the equilibrium state ρ_0 by simply *choosing* a different H_0 to factor out.

unitary propagators of the form $U = \exp(-\mathrm{i}Ht)$:

$$U\rho_0 U^\dagger = U(E + cI_z)U^\dagger = UEU^\dagger + c(UI_zU^\dagger) = E + c(UI_zU^\dagger) \tag{1.40}$$

When describing NMR experiments, it is typical to simply ignore both the E term as well as the proportionality factor c, and focus only on the transformation of the I_z term. Thus, one may define a 'simplified' equilibrium density operator:*

$$\rho_0' = I_z. \tag{1.41}$$

The E term is in fact truly inconsequential, as it cannot ever be transformed into detectable magnetisation. However, the constant c is still relevant: it is manifested in the magnitude of the NMR signal which is ultimately detected. It should be mentioned that ρ_0' is not a true density operator: for example, $\mathrm{Tr}(\rho_0') = 0$ and not 1 as is required for a density operator. Nonetheless, all the physically interesting dynamics of the system such as expectation values are fully contained within ρ_0' (at least up to the proportionality constant c).

1.4 Pulse sequences

It is impossible to provide a full overview of all, or even most, of the major NMR experiments in widespread use; the reader is directed to other books for this purpose.[2,4,5,13,14] I seek only to (briefly) explain the general structure of one- and two-dimensional Fourier transform experiments, and in particular, how the formalisms developed in previous sections can be used to analyse and simulate such experiments.

1.4.1 1D pulse–acquire

Consider the simplest NMR experiment, a 1D ^{1}H pulse–acquire spectrum (section 1.4.1). This consists of a 90° pulse, immediately followed by detection; for convenience, we will first consider the pulse as being applied along the $+y$-axis, i.e. with a phase of $\phi = \pi/2$.

./figures/pp/others/zg_on_y.png

Figure 1.1: 1D ^{1}H pulse–acquire experiment.

*This is similar to the 'deviation' density operator[11,12] which measures how far a density operator deviates from the identity; but I have gone one step further in dropping the factor of c. Note that the alternative term 'reduced density operator' has a different meaning (it refers to the density operator of a subsystem, obtained by taking a partial trace over all other degrees of freedom).

To understand this, we begin with the thermal density operator $\rho_0' = I_z$ (eq. (1.41)) and assume that there is only one spin in the sample, and that the pulse is applied on-resonance. The corresponding Hamiltonian during the pulse is simply $\omega_1 I_y$ (eq. (1.28)). If the duration of the pulse is τ_p, then the density operator immediately following the pulse is given by:

$$\rho = \exp(-\mathrm{i}\omega_1 I_y \tau_\mathrm{p}) I_z \exp(\mathrm{i}\omega_1 I_y \tau_\mathrm{p}) = \cos(\omega_1 \tau_\mathrm{p}) I_z + \sin(\omega_1 \tau_\mathrm{p}) I_x. \tag{1.42}$$

In this case, to obtain a 90° pulse, τ_p is specifically calibrated to ensure that $\omega_1 \tau_\mathrm{p} = \pi/2$, which yields

$$\rho = I_x. \tag{1.43}$$

During the detection period, this term evolves under $H_\mathrm{free} = H_\mathrm{cs} = \omega_0 I_z$. (We use the Schrödinger-picture free Hamiltonian here because the measurement of the NMR signal takes place in the laboratory frame.) At a time t after detection has begun, the density operator is thus:

$$\rho(t) = \exp(-\mathrm{i}\omega_0 I_z t) I_x \exp(\mathrm{i}\omega_0 I_z t) = \cos(\omega_0 t) I_x + \sin(\omega_0 t) I_y. \tag{1.44}$$

The NMR signal derives from both x- and y-magnetisation (M_x and M_y), which are in turn proportional to I_x and I_y by a factor of γ. (If multiple spins are present, then each spin induces its own magnetisation: we would have that $M_x = \sum_i \gamma_i I_{ix}$, and likewise for M_y.) These are then combined to form a complex signal (this process is known as *quadrature detection*):

$$\begin{aligned} s(t) &= M_x(t) + \mathrm{i} M_y(t) && (1.45)\\ &\propto \langle I_x(t) \rangle + \mathrm{i} \langle I_y(t) \rangle \\ &= \mathrm{Tr}[I_x \rho(t)] + \mathrm{i}\,\mathrm{Tr}[I_y \rho(t)] \\ &\propto \cos(\omega_0 t) + \mathrm{i}\sin(\omega_0 t) \\ &= \exp(\mathrm{i}\omega_0 t). && (1.46) \end{aligned}$$

Before the signal is digitised, the NMR spectrometer mixes this with a *reference* RF field oscillating at the transmitter frequency ω_tx. This results in downconversion of the detected frequencies by ω_tx, such that the actual digitised signal oscillates at the offset frequency Ω rather than ω_0 (recall we have chosen $\omega_\mathrm{rot} = \omega_\mathrm{tx}$, so $\omega_0 - \omega_\mathrm{tx} = \omega_0 - \omega_\mathrm{rot} = \Omega$). Therefore, instead of eq. (1.46), the signal we really see is:

$$s(t) \propto \exp(\mathrm{i}\Omega t). \tag{1.47}$$

This result is the same as if we had pretended that during the detection period, ρ evolved under the *interaction-picture* free Hamiltonian $H_{\mathrm{free},I} = H_\mathrm{offset}$; we will henceforth adopt this simplification, even though it is not physically accurate.

In practice, relaxation causes this signal to decay with time; this is frequently modelled as an

exponential, in accordance with the Bloch equations:[15]

$$s(t) = \exp(\mathrm{i}\Omega t)\exp(-t/T_2), \tag{1.48}$$

where T_2 is the transverse relaxation time.* The NMR signal is thus often called a *free induction decay* (FID). Fourier transformation of the FID then yields a spectrum with absorption- and dispersion-mode lineshapes in the real and imaginary parts respectively (fig. 1.2):

$$S(\omega) = \mathscr{F}[s(t)] = \underbrace{\frac{k}{k^2 + (\omega - \Omega)^2}}_{A(\omega;\Omega)} + \mathrm{i}\underbrace{\frac{\Omega - \omega}{k^2 + (\omega - \Omega)^2}}_{D(\omega;\Omega)}, \tag{1.49}$$

where $k = 1/T_2$. The notation $A(\omega;\Omega)$ here means that the spectrum is a function of the frequency ω, but is parametrised by the peak offset Ω. Conventionally, only the real part of the spectrum is displayed, so it is desirable for the real part to contain the absorption-mode lineshape. This provides better resolution due to the narrower lineshape, and is also less affected by cancellation when multiple peaks overlap.

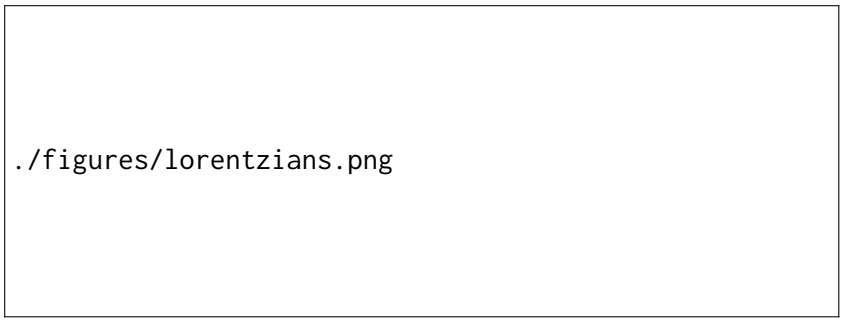

Figure 1.2: **(a)** Absorption-mode lineshape $A(\omega;\Omega = 0)$. **(b)** Dispersion-mode lineshape $D(\omega;\Omega = 0)$. Both lines have been plotted using $k = 1$ Hz.

Strictly speaking, the Lorentzian lineshapes above are only obtained when there is nonzero relaxation during the FID. For example, in the limit $k \to 0$, $A(\omega;\Omega)$ tends to a delta function $\delta(\omega = \Omega)$. However, for simplicity, in this thesis I will drop the relaxation term $\exp(-kt)$ unless absolutely necessary; I will simply pretend that a signal of the form $s(t) = \exp(\mathrm{i}\Omega t)$ is directly Fourier transformed to give $A(\omega;\Omega) + \mathrm{i}D(\omega;\Omega)$.

Consider now changing the initial pulse such that it is applied along the $+x$-axis instead ($\phi = 0$). Repeating the above analysis, we find that the resulting signal will have a phase shift:

$$s'(t) = -\mathrm{i}\exp(\mathrm{i}\Omega t) \tag{1.50}$$

$$\Rightarrow \quad S'(\omega) = \mathscr{F}[s'(t)] = D(\omega;\Omega) - \mathrm{i}A(\omega;\Omega). \tag{1.51}$$

*Transverse (and longitudinal) relaxation are sometimes called spin–spin (and spin–lattice) relaxation, although the continued usage of these terms has been criticised.[3,4,16]

If we were to take the real part of the spectrum here, then we would obtain the undesired dispersion-mode lineshape $D(\omega;\Omega)$. There are two ways of removing this phase shift. The first is to shift the *receiver phase* by ϕ_{rec}, which introduces an extra factor of $\exp(-\text{i}\phi_{\text{rec}})$ to the detected signal: we can thus choose $\phi_{\text{rec}} = 3\pi/2$ in order to cancel out the $-\text{i}$ term in $s'(t)$. Alternatively, the spectrum can be processed through *phase correction*, in which $S(\omega)$ is directly multiplied by a term $\exp(\text{i}\phi_{\text{corr}})$, where ϕ_{corr} is a linear function of the frequency ω:

$$\phi_{\text{corr}} = \phi_{\text{corr}}^{(0)} + \omega\phi_{\text{corr}}^{(1)}. \tag{1.52}$$

$\phi_{\text{corr}}^{(0)}$ and $\phi_{\text{corr}}^{(1)}$ are respectively termed the *zeroth-* and *first-order phase corrections*: in this idealised case, we can simply choose $(\phi_{\text{corr}}^{(0)}, \phi_{\text{corr}}^{(1)}) = (\pi/2, 0)$ to again remove the unwanted phase shift. More realistically, due to instrumental imperfections, both of these values will have to be nonzero in order to ensure that every peak in the spectrum has the correct phase, i.e. is displayed in absorption-mode.

An alternative framework for analysing pulse sequences is to use the ladder operators I_+ and I_- (eq. (1.5)). Using the original example with our initial pulse on $+y$, the density operator immediately after the pulse is:

$$\rho = I_x = \frac{1}{2}(I_+ + I_-), \tag{1.53}$$

and during detection this evolves as:

$$\rho(t) = \cos(\Omega t)I_x + \sin(\Omega t)I_y = \frac{1}{2}\left[\exp(-\text{i}\Omega t)I_+ + \exp(\text{i}\Omega t)I_-\right]. \tag{1.54}$$

To obtain the same signal as previously done in eq. (1.46), we 'detect' the I_- term:

$$s(t) \propto \text{Tr}[I_-\rho(t)] \propto \exp(\text{i}\Omega t), \tag{1.55}$$

which leads to the common assertion that *only quantum coherences of order* -1 *are detectable.* It is true that coherences with orders $p = 0, \pm 2, \pm 3, \ldots$ can never be detected in an FID. However, it is worth pointing out that the 'uniqueness' of -1-coherence is merely a result of how the x- and y-magnetisation are combined to form the complex signal (eq. (1.45)). If we had instead chosen to define $s(t) = M_x(t) - \text{i}M_y(t)$, this would give us $s(t) \propto \exp(-\text{i}\Omega t)$—corresponding to detection of $+1$-coherence—although this alternative does come with the drawback that frequencies must be reversed after Fourier transformation. In any case, we will stick to the established convention of detecting -1-coherence here.

To end this section, it should be pointed out that the complex signal is not obtained as an infinitely-long, continuous function of time, as the treatment above implies. The complex-valued signal is digitised at an interval called the *dwell time*, τ_{dw}, and detection must be stopped after a finite period called the *acquisition time*, τ_{aq}. The Fourier transform being performed is actually

a discrete Fourier transform (DFT), which yields a periodic function $S(\omega)$; its period (in Hz) is given by $1/\tau_{\mathrm{dw}}$.* The NMR spectrum displayed to the user corresponds to one single period of $S(\omega)$, and thus the *spectral width* is also equal to $1/\tau_{\mathrm{dw}}$.† In principle, the periodicity of the DFT means that signals which would ordinarily fall outside of the spectral width would appear at incorrect frequencies in the spectrum.[17] On modern instrumentation, this is no longer the case for direct detection; peaks outside of the spectral width are removed using digital filters. However, *folding* or *aliasing* of peaks in the indirect dimension(s) of multi-dimensional NMR spectra still occurs.

The DFT $S(\omega)$ is also a discrete function itself, and its resolution is given by $1/\tau_{\mathrm{aq}}$. It is possible to extend the effective acquisition time (and thus improve spectral resolution) without actually acquiring more data: this can be done either by *forward linear prediction* of the signal, or by simply adding zeros onto the end of the signal (*zero-filling*).

1.4.2 INEPT and product operators

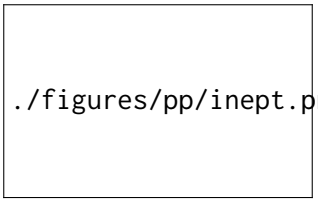

Figure 1.3: INEPT pulse sequence. The delay Δ is set to $1/(4 \cdot {}^{1}J_{\mathrm{CH}})$.

Having tackled a simple single-spin case, we now move to the analysis of coupled spin systems and the development of the so-called 'product operator formalism'.[18] In particular, we look at the INEPT experiment,[19,20] in which magnetisation is transferred from a a nuclide with a high magnetogyric ratio to one with a low magnetogyric ratio through a scalar coupling: for example, from ^{1}H to ^{13}C using the one-bond coupling constant, ${}^{1}J_{\mathrm{CH}}$ (fig. 1.3). Following tradition, the two nuclei are respectively labelled I and S.‡ For a weakly coupled (Schrödinger-picture)§ free Hamiltonian for a weakly coupled system (cf. eqs. (1.12) and (1.13)) is $H_{\mathrm{free}} =$

*The periodicity property of the DFT is equivalent to the Nyquist theorem, which is usually formulated as follows: the sampling rate required to correctly digitise a signal containing frequencies in the range $[0, f_{\mathrm{max}}]$ is $1/(2f_{\mathrm{max}})$. In the main text, it appears as if we have dropped the factor of 2 in the denominator; but in truth this statement of the Nyquist theorem is applicable to *real-valued* signals, and here we have a *complex-valued* signal $s(t)$, which effectively doubles the range of correctly sampled frequencies.

†Frustratingly, the `DW` parameter in Bruker's TopSpin software is actually equal to $\tau_{\mathrm{dw}}/2$. The reason is because this parameter corresponds to the interval between which *real* data is sampled, which is effectively twice as fast as complex-valued sampling.

‡This may seem insensible since I is the *sensitive* and S the *insensitive* nucleus, and indeed, in the original literature[19] the meanings of I and S were swapped. However, this usage has not been consistent,[21] and in modern usage the identification of I as the sensitive nucleus seems to have prevailed.

§This is the last time a Schrödinger-picture Hamiltonian is used in this thesis.

$\omega_{0,I}I_z+\omega_{0,S}S_z+2\pi J_{IS}I_zS_z$. At the very beginning of the sequence, we formally have the equilibrium density operator

$$\rho_0 = \frac{\exp(-\beta\hbar H_{\text{free}})}{\text{Tr}[\exp(-\beta\hbar H_{\text{free}})]} \approx E - \beta\hbar(\omega_{0,I}I_z + \omega_{0,S}S_z + 2\pi J_{IS}I_zS_z), \tag{1.56}$$

using the same approximations as in eq. (1.39). The scalar coupling term can be safely neglected as $2\pi J_{IS}$ is several orders of magnitude smaller than the Larmor frequencies ω_0. After removing the physically irrelevant E term and factoring out a constant of $\beta\hbar B_0$, we end up with:

$$\rho_0' = \gamma_I I_z + \gamma_S S_z. \tag{1.57}$$

This represents equilibrium magnetisation (or *polarisation*) on both spins I and S, in proportion to their magnetogyric ratios. In general, an NMR experiment may manipulate—and ultimately detect—both of these terms. Since unitary evolution according to the Liouville–von Neumann equation is *linear*, in that $U(\rho_1 + \rho_2)U^\dagger = U\rho_1U^\dagger + U\rho_2U^\dagger$, we can treat these two terms separately: we focus first on the spin-I polarisation, $\rho_I = \gamma_I I_z$. The first 90°_x ^{1}H pulse tips this magnetisation into the transverse plane (ignoring off-resonance effects):

$$\rho_I \to \exp[-\text{i}(\pi/2)I_x]\gamma_I I_z \exp[\text{i}(\pi/2)I_x] = -\gamma_I I_y. \tag{1.58}$$

In principle, we could continue in this manner through repeated application of the 'sandwich' formulae (eqs. (1.25) and (1.26), as well as an analogous version for the I_zS_z term). For example, in the Δ delay which follows, we have that

$$\begin{aligned}\rho_I &\to -\gamma_I \exp(-\text{i}H_{\text{free}}\Delta)I_y \exp(\text{i}H_{\text{free}}\Delta) \\ &= -\gamma_I \exp(-\text{i}H_{\text{J}}\Delta) \exp(-\text{i}H_{\text{offset}}\Delta)I_y \exp(\text{i}H_{\text{offset}}\Delta) \exp(\text{i}H_{\text{J}}\Delta) \\ &= \ldots\end{aligned} \tag{1.59}$$

Note that H_{free} here is the interaction-picture free Hamiltonian (eq. (1.22)); and in going from the first to the second line, we can only 'split up' H_{free} into its constituent components H_{offset} and H_{J} because they commute. When performing simulations of NMR experiments, such as those in later chapters, this is precisely what happens, with the slight difference that the Liouville–von Neumann equation (eq. (1.37)) is evaluated numerically rather than symbolically.

When analysing pulse sequences by hand, however, it is far more convenient to use a set of heuristics which summarise the effects of various pulse sequence elements. For example, fig. 1.4 summarises the evolution of a density operator under a single term of the Hamiltonian: as above, since $[H_{\text{offset}}, H_{\text{J}}] = 0$, we only need to consider one term at a time. More high-level rules may be devised as well: for example, during the Δ–$180^\circ_x(I)$, $180^\circ_x(S)$–Δ spin echo which comes next, the J_{IS} interaction in H_{free} is allowed to evolve for a period of 2Δ, but the offset term is *refocused*

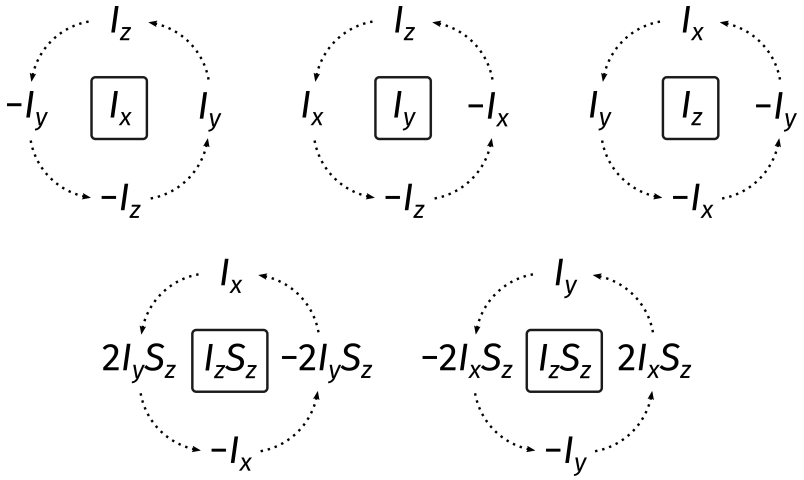

Figure 1.4: Simplified rules for the evolution of product operators under different common Hamiltonians (offset, weak/secular J-coupling, and pulses). These Hamiltonians often have the form ωM where M is some 'base operator', and are applied for a time τ. The boxed operators in the centre of each group refer to M; the initial state is then rotated about this by an angle of $\omega\tau$ to obtain the final state. For example, an 90°_x pulse has the 'base' operator I_x and the angle $\omega\tau = \pi/2$; thus, the initial state I_z would be rotated to $-I_y$.

and can be ignored. (The sign inversion caused by the 180° pulses must also be included.) As per fig. 1.4, this transforms the $-I_y$ term to $-2I_xS_z$ at point (b). The $90^\circ_y(I), 90^\circ_x(S)$ pair of pulses immediately afterwards rotates this to $-2I_zS_y$. These transformations are often denoted with simpler notation:

$$\gamma_I I_z \xrightarrow{90^\circ_x(I)} -\gamma_I I_y \xrightarrow{\Delta-180^\circ_x(I),180^\circ_x(S)-\Delta} -2\gamma_I I_x S_z \xrightarrow{90^\circ_y(I),90^\circ_x(S)} -2\gamma_I I_z S_y \tag{1.60}$$

During the detection period, the term $-2\gamma_I I_z S_y$ evolves as

$$\begin{aligned} -2\gamma_I I_z S_y \xrightarrow{H_{\text{free}}} &-2\gamma_I I_z S_y \cos(\Omega_S t)\cos(\pi J t) + \gamma_I S_x \cos(\Omega_S t)\sin(\pi J t) \\ &- 2\gamma_I I_z S_x \sin(\Omega_S t)\cos(\pi J t) + \gamma_I S_y \sin(\Omega_S t)\sin(\pi J t), \end{aligned} \tag{1.61}$$

from which we extract the complex signal

$$s_I(t) = \langle S_x(t)\rangle + \mathrm{i}\langle S_y(t)\rangle = \frac{\gamma_I}{2\mathrm{i}}\{\exp[\mathrm{i}(\Omega_S + \pi J_{IS})t] - \exp[\mathrm{i}(\Omega_S - \pi J_{IS})t]\}. \tag{1.62}$$

After Fourier transformation, the resulting spectrum has two peaks with opposite phase and have the frequencies $\Omega_S \pm \pi J_{IS}$; because of the factor of $1/(2\mathrm{i})$, the real part of the spectrum will contain dispersion-mode signals (fig. 1.5a). If desired, zeroth-order phase correction can be performed here, yielding instead a pair of absorption-mode signals still with opposite phases (fig. 1.5b). In either case, this is termed an *antiphase* doublet; the product operators which give rise to it ($2I_zS_x$ and $2I_zS_y$) are said to be antiphase with respect to spin I. Importantly, the amplitude of the signal scales as γ_I rather than γ_S, as it would if we had started from equilibrium

spin-S magnetisation: this signal enhancement by $|\gamma_I/\gamma_S|$ is the entire reason for the INEPT experiment.

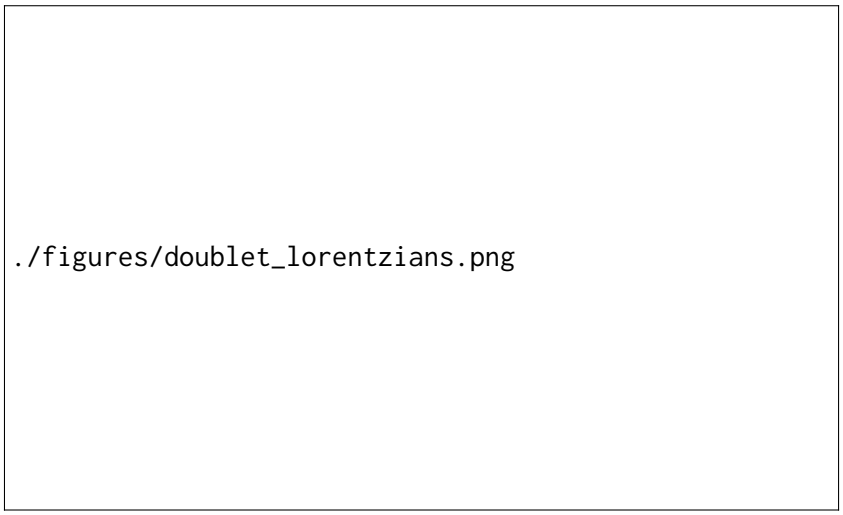

Figure 1.5: Peak shapes of a doublet. **(a)** Antiphase, dispersion-mode. **(b)** Antiphase, absorption-mode. **(c)** In-phase, dispersion-mode. **(d)** In-phase, absorption-mode.

Of course, this is only half of the picture; we have not considered what happens to the other part of the magnetisation, namely $\rho_S = \gamma_S S_z$. Clearly, this is unaffected by the initial $90^\circ_x(I)$ pulse and the first Δ delay. The $180^\circ_x(S)$ pulse inverts it, and the final $90^\circ_x(S)$ pulse in fact transforms it into observable S-magnetisation:

$$\gamma_S S_z \xrightarrow{90^\circ_x(I)-\Delta} \gamma_S S_z \xrightarrow{180^\circ_x(I),180^\circ_x(S)-\Delta} -\gamma_S S_z \xrightarrow{90^\circ_y(I),90^\circ_x(S)} \gamma_S S_y \tag{1.63}$$

This term produces *in-phase* spin-S magnetisation during the detection period (where the two components of the doublet have the same phase):

$$s_S(t) = \frac{\mathrm{i}\gamma_S}{2}\{\exp[\mathrm{i}(\Omega_S + \pi J_{IS})t] + \exp[\mathrm{i}(\Omega_S - \pi J_{IS})t]\}, \tag{1.64}$$

Because of the factor of i, the real part of the spectrum will contain a dispersion-mode doublet (fig. 1.5c). The signal actually measured by the spectrometer is $s(t) = s_I(t) + s_S(t)$; and the spectrum is a weighted sum of in-phase and antiphase magnetisation. This leads to potentially unwanted phase distortions in the spectrum, which one would prefer to suppress.

This can be accomplished through the technique of *phase cycling*, where pulse and receiver phases are changed in concert and the resulting FIDs summed in order to select for a particular signal. In this case, the INEPT experiment is performed twice, once with the phases as given in fig. 1.3, and once where the initial $90^\circ_x(I)$ pulse is replaced with a $90^\circ_{\bar{x}}(I)$ pulse. The first of these gives us the same signals as above. However, inverting the initial I pulse leads to s_I acquiring a minus sign, because the initial I_z term is rotated to I_y instead of $-I_y$. On the other hand, the signal component

s_S is unaffected by this pulse and thus does not experience a change of sign. The two FIDs we record are thus as follows:

$$s_1(t) = s_I(t) + s_S(t) \tag{1.65}$$

$$s_2(t) = -s_I(t) + s_S(t) \tag{1.66}$$

Simply taking the difference of these two FIDs yields a signal where the desired s_I has been accumulated and s_S has been cancelled out. In practice, instead of subtracting the two signals, it is typical to shift the receiver phase ϕ_{rec} by 180° in the second experiment: this introduces a phase shift of $\exp(-\mathrm{i}\pi) = -1$ to the signal, and the two signals can now be *added* together instead of subtracted to cancel out s_S. We can express this as $\phi_x = \phi_{\text{rec}} = (0, \pi)$, or more commonly, $\phi_1 = \phi_{\text{rec}} = (x, -x)$ because the phases $(0, \pi)$ correspond to the $+x$- and $-x$-axes respectively.

The 'simplified' analysis of pulse sequences shown in eqs. (1.60) and (1.63) is often called '*product operator*' analysis,[18] because the underlying two-spin operators are products of single-spin Cartesian operators. Although this is often touted as being 'simpler' than full density operator calculations, it is really just a shorthand which masks the quantum mechanical theory developed in this chapter:

$$\underbrace{I_z \xrightarrow{90^\circ_x(I)} -I_y}_{\textit{product operator}} \quad \Longleftrightarrow \quad \underbrace{\exp(-\mathrm{i}I_x\pi/2) I_z \exp(\mathrm{i}I_x\pi/2) = -I_y}_{\textit{density operator}} \tag{1.67}$$

Since the operators $\{E, I_x, I_y, I_z\}$ form a complete basis for a single-spin system, their products (i.e. product operators) likewise form a complete basis for multiple-spin systems, and so *any* density matrix for a multiple-spin system may be expressed as a linear combination of product operators. Strictly speaking, the use of product operators therefore does not actually sacrifice any power in and of itself. However, the heuristics such as those in fig. 1.4 *are* limiting, in that the evolution under some Hamiltonians—for example, strong coupling $\mathbf{I} \cdot \mathbf{S}$, or pulses for off-resonant spins where H is a sum of I_x and I_z—cannot be neatly captured in such a pictorial form.

1.4.3 2D NMR: HSQC

The use of coherence orders is particularly effective in the analysis of modern 2D NMR experiments, which make use of multiple different techniques to select for particular *coherence transfer pathways* (CTPs). A full discussion of this is beyond the scope of this thesis. Nevertheless, the analysis of a 2D ^{1}H–^{13}C HSQC experiment (fig. 1.6) is given here as an example to illustrate the concepts of CTP selection through *phase cycling* and gradients, as well as the related issue of quadrature detection in indirect dimensions.

The HSQC experiment seeks to only detect protons directly bonded to ^{13}C; all other protons

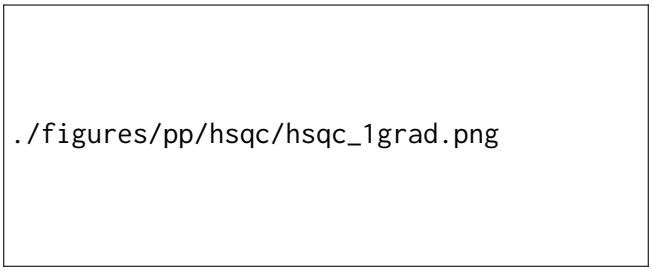

Figure 1.6: A typical echo–antiecho HSQC pulse sequence (the symbols are explained in the *Preface*). The pulse phase ϕ_1 and the receiver phase ϕ_{rec} are together alternated between 0 and π; this is typically denoted as $\phi_1 = \phi_{\text{rec}} = (x, -x)$ as these phases correspond to the $+x$- and $-x$-axes. The delay Δ is set to $1/(4 \cdot {}^1J_{\text{CH}})$. The gradient amplitudes are chosen such that $|g_1/g_2| = \gamma_{\text{H}}/\gamma_{\text{C}} \approx 4$. Echo–antiecho CTP selection is carried out by inverting the sign of g_2.

must be suppressed. We first show how pulsed field gradients and phase cycling allow the *desired* signal to be obtained.

This is technically only appropriate for an isolated methine (i.e. CH) group. The analysis which proceeds, however, is identical for methylene and methyl groups, which would be I_2S and I_3S systems respectively. More unsound is the complete neglect of H–H coupling. Luckily, this does not pose a serious problem here: it essentially leads to a small loss of signal. However, for other experiments it may be necessary to account for ${}^nJ_{\text{HH}}$: for example, it causes artefacts in the sensitivity-enhanced HSQC, as will be discussed in section 4.3.1. In general, this illustrates the point that one should choose the *simplest possible system* (but not one any simpler) to analyse a pulse sequence.

- CTP selection through gradients, mathematical requirement for CTP to be refocused
- Quadrature detection in F_1 (ugh)
- Composite coherence order[22,23]
- phase cycling to cancellation of unwanted peaks (e.g. arising from ^{12}C-bound ^{1}H)
- explain why phase cycling (on its own) isn't really used for CTP selection any more

1.5 References

(1) Ernst, R. R.; Bodenhausen, G.; Wokaun, A., *Principles of Nuclear Magnetic Resonance in One and Two Dimensions*; Clarendon Press: Oxford, U.K., 1987.

(2) Cavanagh, J.; Fairbrother, W. J.; Palmer III, A. G.; Rance, M.; Skelton, N. J., *Protein NMR Spectroscopy: Principles and Practice*, 2nd ed.; Academic Press: Burlington, Mass., 2007.

(3) Levitt, M. H., *Spin Dynamics: Basics of Nuclear Magnetic Resonance*, 2nd ed.; Wiley: Chichester, U.K., 2008.
(4) Keeler, J., *Understanding NMR Spectroscopy*, 2nd ed.; Wiley: Chichester, U.K., 2010.
(5) Hore, P. J.; Jones, J. A.; Wimperis, S., *NMR: The Toolkit, How Pulse Sequences Work*, 2nd ed.; Oxford University Press: Oxford, U.K., 2015.
(6) Sakurai, J. J.; Napolitano, J., *Modern Quantum Mechanics*; Cambridge University Press: Cambridge, U.K., 2021.
(7) Blum, K., *Density Matrix Theory and Applications*; Springer: Heidelberg, 2012.
(8) Cohen-Tannoudji, C.; Diu, B.; Laloë, F., *Quantum Mechanics*, 2nd ed.; Wiley: Weinheim, Germany, 2020.
(9) Breuer, H.-P.; Petruccione, F., *The Theory of Open Quantum Systems*; Oxford University Press: Oxford, U.K., 2002.
(10) Lidar, D. A. Lecture Notes on the Theory of Open Quantum Systems, 2019, DOI: 10.48550/arxiv.1902.00967.
(11) Chuang, I. L.; Gershenfeld, N.; Kubinec, M. G.; Leung, D. W. Bulk quantum computation with nuclear magnetic resonance: theory and experiment. *Proc. R. Soc. Lond. A* **1998**, *454*, 447–467, DOI: 10.1098/rspa.1998.0170.
(12) Jones, J. A. Quantum computing with NMR. *Prog. Nucl. Magn. Reson. Spectrosc.* **2011**, *59*, 91–120, DOI: 10.1016/j.pnmrs.2010.11.001.
(13) Findeisen, M.; Berger, S., *50 and More Essential NMR Experiments: A Detailed Guide*; Wiley: Weinheim, 2013.
(14) Claridge, T. D. W., *High-Resolution NMR Techniques in Organic Chemistry*, 3rd ed.; Elsevier: Amsterdam, 2016.
(15) Bloch, F. Nuclear Induction. *Phys. Rev.* **1946**, *70*, 460–474, DOI: 10.1103/physrev.70.460.
(16) Gupta, A.; Stait-Gardner, T.; Price, W. S. Is It Time to Forgo the Use of the Terms "Spin–Lattice" and "Spin–Spin" Relaxation in NMR and MRI? *J. Phys. Chem. Lett.* **2021**, *12*, 6305–6312, DOI: 10.1021/acs.jpclett.1c00945.
(17) Turner, C. J.; Hill, H. D. W. Artifacts in quadrature detection. *J. Magn. Reson.* **1986**, *66*, 410–421, DOI: 10.1016/0022-2364(86)90185-x.
(18) Sørensen, O. W.; Eich, G. W.; Levitt, M. H.; Bodenhausen, G.; Ernst, R. R. Product operator formalism for the description of NMR pulse experiments. *Prog. Nucl. Magn. Reson. Spectrosc.* **1984**, *16*, 163–192, DOI: 10.1016/0079-6565(84)80005-9.
(19) Morris, G. A.; Freeman, R. Enhancement of nuclear magnetic resonance signals by polarization transfer. *J. Am. Chem. Soc.* **1979**, *101*, 760–762, DOI: 10.1021/ja00497a058.

(20) Morris, G. A. Sensitivity enhancement in nitrogen-15 NMR: polarization transfer using the INEPT pulse sequence. *J. Am. Chem. Soc.* **1980**, *102*, 428–429, DOI: 10.1021/ja00521a097.

(21) Pines, A.; Gibby, M. G.; Waugh, J. S. Proton-Enhanced Nuclear Induction Spectroscopy. A Method for High Resolution NMR of Dilute Spins in Solids. *J. Chem. Phys.* **1972**, *56*, 1776–1777, DOI: 10.1063/1.1677439.

(22) John, B. K.; Plant, D.; Heald, S. L.; Hurd, R. E. Efficient detection of CαH–HN correlations in proteins using gradient-enhanced ^{15}N HMQC-TOCSY. *J. Magn. Reson.* **1991**, *94*, 664–669, DOI: 10.1016/0022-2364(91)90158-p.

(23) Mitschang, L.; Ponstingl, H.; Grindrod, D.; Oschkinat, H. Geometrical representation of coherence transfer selection by pulsed field gradients in high-resolution nuclear magnetic resonance. *J. Chem. Phys.* **1995**, *102*, 3089–3098, DOI: 10.1063/1.468618.

Chapter 2

Pure shift NMR

2.1 Introduction

Pure shift NMR refers to the technique of acquiring NMR spectra free of multiplet structure, such that every chemical environment gives rise to a singlet.[1] To accomplish this, the effect of both heteronuclear and homonuclear couplings must be removed. If only heteronuclear couplings exist, as is typically the case with dilute nuclei such as ^{13}C, then this is trivially accomplished by decoupling during the acquisition period. However, removing *homonuclear* couplings is a substantially more difficult task, as decoupling cannot be applied on the same radiofrequency channel as the signal is being detected on. Therefore, in practice, the term 'pure shift' is only used in the context of solution-state homonuclear decoupling. Although pure shift techniques can be applied to any NMR-active nucleus, ^{1}H is by far the most important, due to the abundance of ^{1}H–^{1}H couplings in typical molecules.

2.2 Direct optimisation of PSYCHE

Stuff that didn't quite work very well.

2.3 PSYCHE with variable number of saltire pulses

Blah.

2.4 Time-reversal method

Blah.

2.5 'Discrete PSYCHE'

Blah.

2.6 Ultrafast PSYCHE-iDOSY

Blah.

2.7 References

(1) Zangger, K. Pure shift NMR. *Prog. Nucl. Magn. Reson. Spectrosc.* **2015**, *86-87*, 1–20, DOI: 10.1016/j.pnmrs.2015.02.002.

Chapter 3

POISE

3.1 Introduction

Including optimisation theory.

3.2 Implementation

Blah.

Flowchart.

Python 3. Blah.

3.3 Applications

3.3.1 Pulse width calibration

`popt` vs `pulsecal`

3.3.2 Ernst angle optimisation

Maths

3.3.3 NOE mixing time

Stuff

3.3.4 ASAP-HSQC excitation delay

INEPT

3.3.5 HMBC low-pass J-filter

Artefacts.

3.3.6 Inversion–recovery

Stuff

3.3.7 Ultrafast NMR

EPSI gradient imbalance

3.3.8 PSYCHE pure shift NMR

J-refocusing

3.3.9 Water suppression

Mouse

3.3.10 Diffusion NMR

Automated DOSY

3.4 POISE for ESR

Blah

3.5 Conclusion

It's amazing, give us a like and subscribe plz

Chapter 4

NOAH

4.1 Introduction

NOAH.[1–9]

4.2 GENESIS: automated pulse programme creation

Probably makes sense to start with this; that way everything else can be placed in context.

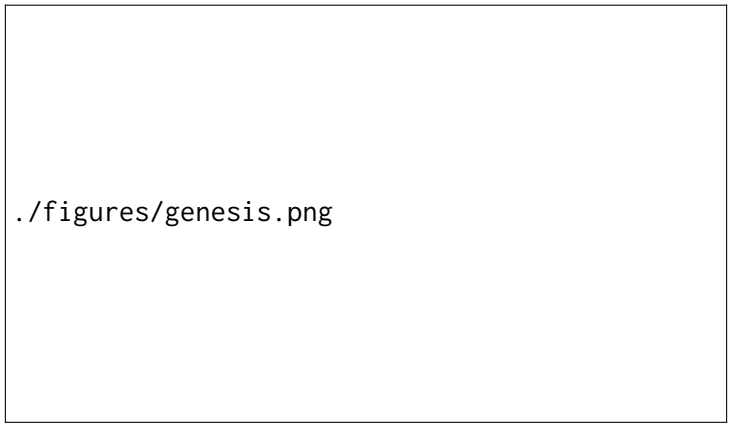

Figure 4.1: What font am I? $y = ax^2 + bx + c$ *M*M Lorem ipsum dolor sit amet, consectetur adipiscing elit, sed do eiusmod tempor incididunt ut labore et dolore magna aliqua. Ut enim ad minim veniam, quis nostrud exercitation ullamco laboris nisi ut aliquip ex ea commodo consequat. Duis aute irure dolor in reprehenderit in voluptate velit esse cillum dolore eu fugiat nulla pariatur. Excepteur sint occaecat cupidatat non proident, sunt in culpa qui officia deserunt mollit anim id est laborum.

4.3 Discussion of individual modules

4.3.1 Sensitivity-enhanced HSQC

Stuff.

4.3.2 HSQC-TOCSY

Blah.

Blah2.

4.3.3 HSQC-COSY

Blah.

4.3.4 2DJ and PSYCHE

cnst37 scaling

SAPPHIRE

4.3.5 DQF-COSY

States vs EA

4.3.6 HMQC

Wing artefacts

4.3.7 HMBC

$^{1}J_{\mathrm{CH}}$ artefacts.

Also ^{15}N HMBC. Blah.

4.3.8 ADEQUATE

...has inadequate sensitivity

4.4 Solvent suppression in NOAH

Blah.

4.5 NOAH with short relaxation delays (???)

Blah.

4.6 Parallel NOAH supersequences

This should probably be a short chapter.

List of figures

List of tables

Appendix A

Other work

A.1 NMR plotting in Python

https://github.com/yongrenjie/penguins

A.2 Citation management

https://github.com/yongrenjie/abbotsbury

A.3 Group website and pulse programming tutorials

https://foroozandehgroup.github.io